Computers in Biology and Medicine 184 (2025) 109380

Contents lists available at ScienceDirect

Computers in Biology and Medicine

journal homepage: www.elsevier.com/locate/compbiomed

Design of patient-specific mandibular reconstruction plates and a hybrid scaffold

Sait Emre Dogan [a], Cengizhan Ozturk [a], Bahattin Koc [b,c,*]

[a] Bogazici University, Institute of Biomedical Engineering, Istanbul, 34684, Turkiye
[b] 3D Bioprinting Laboratory, Sabanci University Nanotechnology Research and Application Center, Istanbul, 34956, Turkiye
[c] Faculty of Engineering and Natural Sciences, Sabanci University, Istanbul, 34956, Turkiye

ARTICLE INFO

Keywords:
Mandibular segmental defects
Reconstruction plate
Voronoi
FEA
Mandibular reconstruction plate

ABSTRACT

Background: Managing segmental mandibular defects remains challenging, requiring a multidisciplinary approach despite the remarkable progress in mandibular reconstruction plates, finite element methods, computer-aided design and manufacturing techniques, and novel surgical procedures. Complex surgeries require a comprehensive approach, as using only reconstruction plates or tissue scaffolds may not be adequate for optimal results. The limitations of the treatment options should be investigated towards a patient-specific trend to provide shorter surgery time, better healing, and lower costs. Integrated hybrid scaffold systems are promising in improving mechanical properties and facilitating healing. By combining different materials and structures, hybrid scaffolds can provide enhanced support and stability to the tissue regeneration process, leading to better patient outcomes. The use of such systems represents a significant advancement in tissue engineering and a wide range of medical procedures.

Materials and Methods: A head and neck computed tomography (CT) data of a patient with odontogenic myxoma was used for creating a three-dimensional (3D) mandible model. Virtual osteotomies were performed to create a segmental defect model, including the angulus mandibulae region. The first mandibular reconstruction plate was designed. Finite elemental analyses (FEA) and topology optimizations were performed to create two different reconstruction plates for different treatment scenarios. The FEA were performed for the resulting two plates to assess their biomechanical performance. To provide osteoconductive and osteoinductive properties a scaffold was designed using the defect area. A biomimetic Tricalcium phosphate-Polycaprolactone (TCP-PCL) hybrid bone scaffold enhanced with Hyaluronic acid dipping was manufactured.

Results: The results of the in-silico analysis indicate that the designed reconstruction plates possess robust biomechanical performance and demonstrate remarkable stability under the most rigorous masticatory activities. Using the Voronoi pattern decreased the mass by %37 without losing endurance. Using reconstruction plates and hybrid scaffolds exhibits promising potential for clinical applications, subject to further in vivo and clinical studies.

1. Introduction

The management of trauma and cancer-related tissue or organ losses remains a significant challenge from both health and economic standpoints [1–4]. Reconstructing lost tissues, particularly critical-size and load-bearing craniofacial defects, poses a complex and multidisciplinary challenge. Segmental mandibular defects, given the intricate nature of the mandible's anatomy, present a particularly problematic scenario. Presently, the management of such defects involves the transplantation of tissues, medical implants, or a combination of both [5–7].

This study introduces a novel hybrid scaffold system that combines a patient-specific reconstruction plate with a patient-specific scaffold to address the challenges in tissue engineering. The primary objective of this system is to enhance tissue regeneration by leveraging the benefits of both components. Despite advancements in regenerative medicine and the use of reconstruction plates, challenges such as limited donor supply, defect size, compromised healing, and complex anatomy persist [8–11]. The standard treatment for critical-size segmental defects is the free-flap procedure, which, however, has its own drawbacks, such

* Corresponding author.
E-mail addresses: sait.dogan@std.bogazici.edu.tr (S.E. Dogan), cozturk@bogazici.edu.tr (C. Ozturk), bahattinkoc@sabanciuniv.edu (B. Koc).

https://doi.org/10.1016/j.compbiomed.2024.109380
Received 1 April 2024; Received in revised form 24 October 2024; Accepted 6 November 2024

as morbidity and the need for additional surgeries. In these surgeries, reconstruction plates are used to fixate mandibular segments and grafts.

The use of titanium, particularly the Ti6Al4V alloy, has revolutionized reconstruction due to its corrosion resistance and biocompatibility [12,13]. However, its higher elasticity modulus can lead to stress shielding [14–16]. Newer alloys like Ti6Al7Nb offer comparable biocompatibility but are more expensive, resulting in the continued widespread use of Ti6Al4V [13,17,17–21]. In this study, Ti6Al4V is used for designing reconstruction plates.

Reconstruction plate designs have evolved from non-rigid wiring to standard, non-locking, and locking plates, with the advent of patient-specific implants made possible through additive manufacturing [22–25]. However, complications still occur, particularly with mandibular discontinuity defects containing the ramus region, which have higher failure rates [26]. This study uses a segmental mandibular defect covering the ramus and angulus regions to simulate a challenging clinical scenario.

In practice, plate bending can lead to uneven stress distribution and fractures, while screw loosening is dependent on factors such as bone quality and stress [14,14,26–29]. Patient-specific implants can help address plate fractures, and finite element analysis (FEA) can optimize plate topology [30–32]. Detailed biomechanical analyses are essential to simulate real-world scenarios [33–36]. While reconstruction plates can stabilize mandible segments, they do not ensure bone healing, thus necessitating scaffolds with osteoinductive and osteoconductive properties.

The concept of biomimetic tissue scaffolds has been explored since the 1990s, with the idea evolving alongside additive manufacturing techniques [10,37,38]. Scaffolds can serve as alternatives to free flaps when additional surgeries are not feasible, offering personalized solutions [39–43]. Natural scaffolds provide biocompatibility but lack mechanical strength, while synthetic scaffolds offer superior mechanical properties but lower biocompatibility [42–47]. Hybrid scaffolds combining the advantages of both have emerged, mimicking the composition of native bone [44–46,48–52].

The use of hybrid scaffold systems, which combine reconstruction plates and scaffolds, has the potential to reduce surgery time and improve healing. This study introduces a hybrid scaffold system that combines patient-specific reconstruction plates with a tricalcium phosphate-polycaprolactone (TCP-PCL) scaffold, tailored to maximize effectiveness and healing. The TCP-PCL scaffold was designed to mimic the native mandible defect site and was optimized for vascularization and bone formation, utilizing a commercially available bioprinter. Furthermore, advanced plates were designed for different requirements, including a hollowed plate for screening applications and a Voronoi plate for load-bearing purposes. The Voronoi pattern, utilized for the first time in this study, reduced the plate's mass while maintaining its strength. Static structural analyses demonstrated that all designed plates were capable of withstanding masticatory forces.

2. Materials and methods

2.1. Retrieving medical images and segmentation

A head and neck CT scan of a male patient with odontogenic myxoma, a locally aggressive and benign neoplasm, was used to segment the mandible. DICOM (Digital Imaging and Communications in Medicine) was imported to the Materialise Mimics 25.0®(Mimics, Materialise Co., Leuven, Belgium). Cortical and trabecular bone regions were segmented separately, with suitable Hounsfield unit (HU) values benefiting the literature and the software (Boolean operation), specifically for this case, since there are no exact values that are valid universally [53–55]. Two models were segmented for FEA.

The first is a basic model that assumes that the entire mandible consists of cortical bone for the first analysis. The second model separately reflects the cortical and trabecular bones. The "Finite Element Analysis and Topology Optimization" section will elucidate the underlying reasoning for adopting this approach. The segmented models were exported in STL (Standard Tessellation Language) format.

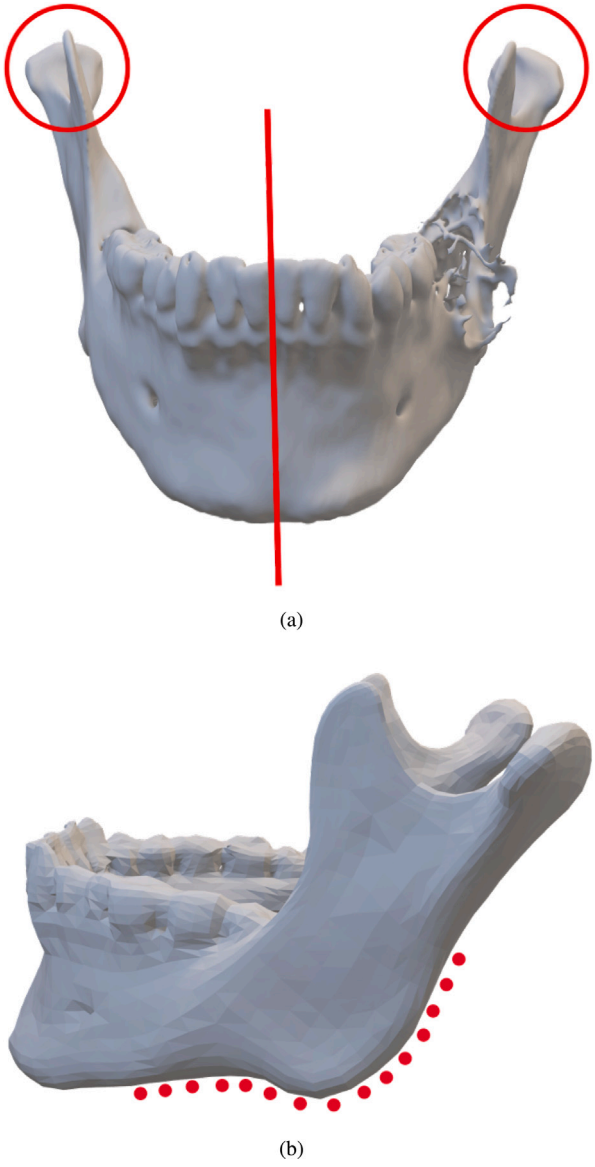

Fig. 1. Some of the anatomical landmarks on the original model used in the mirroring process(a), newly formed border benefiting the line followed through the posterior border of the mandibular ramus mandibulae, angulus mandibulae, and basis mandibulae(b).

2.2. Model design

The STL files were imported into Materialise 3-Matic 17.0® (3-Matic, Materialise Co., Leuven, Belgium) to perform virtual osteotomies and design reconstruction plates. A virtual segmental resection was applied to remove the defect area. Subsequently, a mirroring operation was performed, taking into account anatomical and craniometric landmarks such as fovea pterygoidea, condylion laterale, condylion mediale, spina mentalis, and protuberantia mentalis to ensure the accuracy of the new model's location in the spatial plane. Also, mirroring was checked with an outer line that followed the posterior border of the ramus mandibulae, angulus mandibulae, and basis mandibulae to ensure that the continuity of the bone was protected in the new design. This approach provided increased precision and aesthetics. Figs. 1 and 2 depict the original mandible and the mirrored model with used anatomical landmarks and referential entities. Table 1 shows the definition of reference entities.

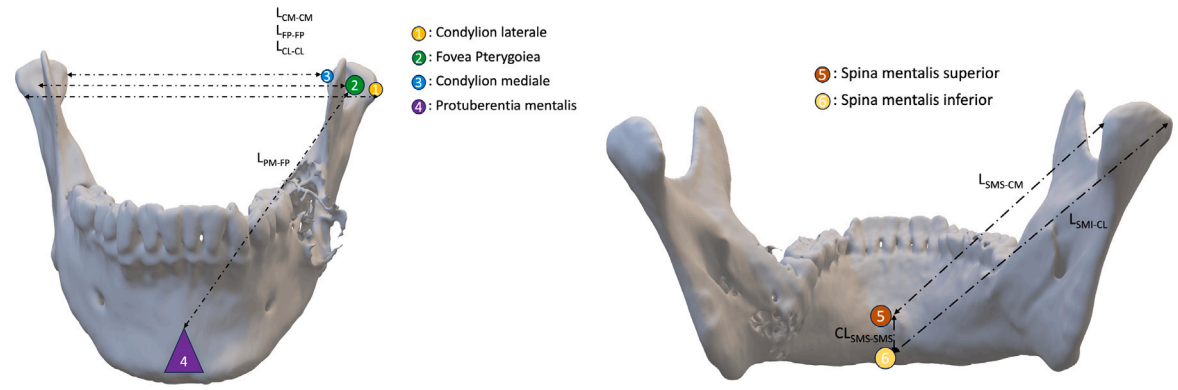

Fig. 2. Anatomical landmarks and referential entities on the original model used in the mirroring process. Conylion regions, fovea pterygoidea, protuberentia mentalis (a); Spina mentalis regions and condylion regions(b).

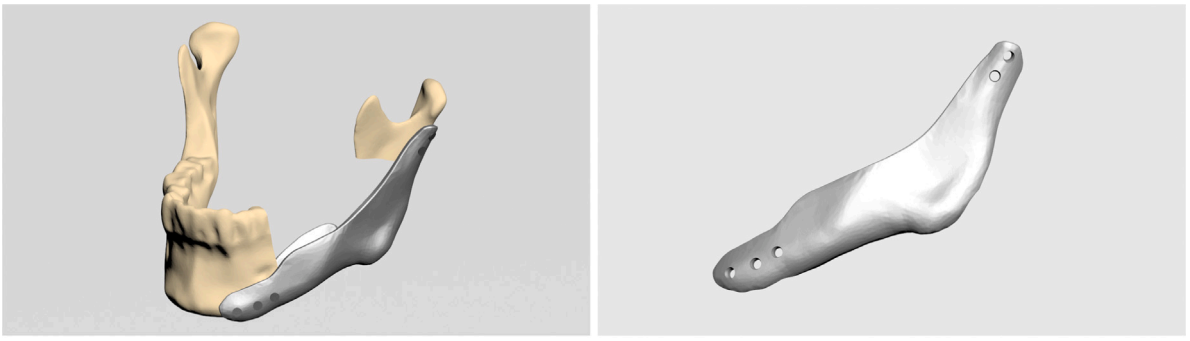

Fig. 3. The first plate design for topology optimization and light-weighting(a), the first model for FEA (b).

Table 1
The definition of referential entities.

Referential entities	Definition
L_{CM-CM}	The distance between right and left condylion mediale
L_{FP-FP}	The distance between right and left fovea pterygoidea
L_{CL-CL}	The distance between right and left condylion laterale
L_{PM-FP}	The distance between protuberentia mentalis and fovea pterygoidea
L_{SMS-CM}	The distance between spina mentalis superiore and condylion mediale
L_{SMI-CL}	The distance between spina mentalis inferiore and condylion laterale
$CL_{SMS-SMI}$	Connecting line between spina mentalis superiore and spina mentalis inferiore

On the mirrored model, a related region was selected considering the roots of the remaining teeth and Champhy's stress lines to provide stable fixation and decrease the chances of the stress shielding effect. The data on the efficiency of following stress lines in segmental defects is limited since it was a technique developed for reconstructing fracture cases. However, the idea behind the technique is to use biomechanically favorable parts of the bone in which less stability would be sufficient [56,57]. Selected area was then offset, and screw holes were added. Medical publications have no agreement on the perfect thickness of mandibular reconstruction plates or the screw diameters. However, the literature indicates that many surgeons prefer to use 2–2.5 mm thick reconstruction plates for internal rigid fixation [58]. Below 2 mm was correlated with an increased fracture rate [16]. For this study, a 2.5 mm thick plate was used. On the lingual side, the plate border was placed below the mylohyoid line to allow the plate to hold the scaffold without obstructing muscle reconstruction during surgery. Plate borders were elongated medially and distally to minimize the stress shielding effect. Fixation screws with a diameter of 2.8 mm and lengths of 7.5 and 10 mm were designed for use considering the size of the defect. Since the plate follows the mandible borders, no gaps exist between the plate and the bone, which is beneficial for stability. The first reconstruction plate and the defect model were then exported. Fig. 3 illustrates the defect model and first reconstruction plate design that will be used for topology optimization.

2.3. Optimization of the geometry

The first reconstruction plate and the defect model were imported to ANSYS (ANSYS Inc., USA) to perform static structural analysis (FEA). The choice of material for plates was Ti6Al4V, and for screws was titanium. The behavior of the plate was more important at this step. Therefore, the first model consists of cortical bone for ease of study. The material properties were provided from various literature, shown in Table 2 [33,34,59,60]. There are six main masticatory tasks used to assess the biomechanical performance of the maxillofacial reconstruction plates. Previous literature expresses that two tasks caused prominent stress levels in the angulus mandibulae region. Constrained right molars and constrained left molars [33–35,61]. Therefore, for the ease of the study, only these tasks were used for FEA. Tie-constraint screws were used to avoid relative motions between the screw-bone

Table 2
Material properties used in the FEA Analysis.

	Elastic modulus (GPa)	Poisson's ratio	Yield strength (MPa)	Young's modulus
Ti-6Al-4V	115	0.323	107	115
Cortical Bone	12	0.3	88	96.2
Trabecular Bone	1–2	0.3	3.9	96.2
Titanium Screws	110	0.3	850	116

Table 3
The muscle forces performing clenching tasks. Raw data was acquired from the literature [61]. Muscular forces: SM-superficial masseter, DM-deep masseter, MP-medial pterygoid, ILP-inferior lateral pterygoid, AT-anterior temporalis, MT-middle temporalis, PT-posterior temporalis.

Clenching tasks	Side	Direction	Muscular force							Constraint
			SM	*DM*	*MP*	*AT*	*MT*	*PT*	*ILP*	
Right Unilateral Molar Clench	Right	Force	137.1	58.8	146.9	115.4	63.1	44.6	20.1	**Constrained right molars**
		Fx	−28.4	−32.1	71.4	−17.2	−14.0	−9.3	12.6	
		Fy	121.2	44.5	116.1	114.0	52.8	21.1	−3.5	
		Fz	57.4	−21.0	54.8	5.1	−31.5	−38.1	15.2	
	Left	Force	114.2	49.0	104.9	91.7	64.0	29.5	43.5	
		Fx	23.6	26.7	−51.0	13.7	14.2	6.1	−27.4	
		Fy	101.0	37.1	83.0	90.5	53.6	14.0	−7.6	
		Fz	47.9	−17.5	39.1	4.0	−32.0	−25.2	32.9	
Left Unilateral Molar Clench	Right	Force	114.2	49.0	104.9	91.7	64.0	29.5	43.5	
		Fx	−23.6	−26.7	51.0	−13.7	−14.2	−6.1	27.4	
		Fy	101.0	37.1	83.0	90.5	53.6	14.0	−7.6	
		Fz	47.9	−17.5	39.1	4.0	−32.0	−25.2	32.9	**Constrained left molars**
	Left	Force	137.1	58.8	146.9	115.4	63.1	44.6	20.1	
		Fx	28.4	32.1	−71.4	17.2	14.0	9.3	−12.6	
		Fy	121.2	44.5	116.1	114.0	52.8	21.1	−3.5	
		Fz	57.4	−21.0	54.8	5.1	−31.5	−38.1	15.2	

and screw-plate surfaces and provide more detailed information on stresses on the plate [61–65]. The muscle forces during the masticatory tasks are provided in Table 3. The boundary conditions illustrated in Fig. 4 were adjusted according to the previous literature and the patient anatomy [33–35,61]. The governing equation used for FEA is provided below. It represents the governing equation for a damped harmonic oscillator, which is often used in finite element analysis (FEA) for dynamic systems. In this study, FEA was performed under static conditions; hence, the acceleration and velocity values were considered zero.

$$F = m\ddot{x} + c\dot{x} + kx$$

- F = External force applied to the system
- m = Mass of the system
- $\ddot{x}$ = Acceleration
- c = Damping coefficient
- $\dot{x}$ = Velocity
- k = Stiffness of the system
- x = Displacement

Since the FEA was performed for static conditions;

- $\ddot{x} = 0$ and $\dot{x} = 0$

$$F = kx$$

The results of the first analysis, shown in Figs. 6, 7 and Support Data, illustrate the areas with the most stress. There were no areas with a force that exceeded the maximum strength levels of the material. This result was expected since the reconstruction plates used in real cases have much less volume. However, the first design aimed to find the maximum stress areas and perform topology optimization and light-weighting.

2.4. Finite elemental analysis and topology optimization

Upon analysis of the results, the areas of highest stress in the reconstruction plate were identified through a finite element analysis (FEA) of extreme human clenching forces on the angulus mandibulae region. This allowed for the creation of two distinct designs aimed at addressing different clinical needs.

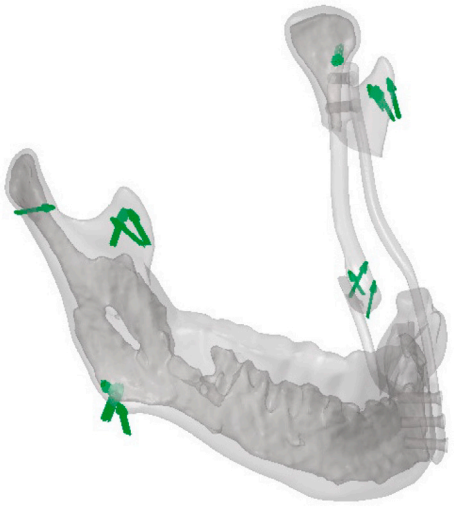

Fig. 4. Boundary conditions, segmented trabecular, and cortical bone are shown on the hollowed model.

The first design involved modifying the plate to create a hollow structure, which improved the visibility of the defect area while retaining its capacity to support a scaffold. This hollowed configuration introduced new borders around high-stress zones, with a 2.5 × 2.5 mm diameter line tracing the outer layer. The central section was intentionally left open to facilitate cancer recurrence screening following surgical intervention.

For the second design, Voronoi tessellation was utilized to construct a lightweight structure. Voronoi diagrams, a dual formulation of triangulations, have been widely used in various optimization and design tasks due to their inherent properties of space partitioning in the previous literature [66,67]. It has been used on cranial implants

due to its customizable nature and anisotropic properties [68–70]. The present study follows a similar but improved approach.

The Voronoi structure was optimized by strategically positioning attractor points in areas of high stress detected in the finite element analysis (FEA) to increase material density, while fewer points were placed in low-stress areas to reduce material usage. The centers of attraction, which define the points for Voronoi tessellation, were objectively determined based on the stress patterns revealed by the FEA. High-stress regions, identified through simulation, served as the primary locations for these attractor points, ensuring enhanced support and stability where it was most needed.

This method resulted in a lightweight design that did not compromise the load-bearing capacity of the reconstruction plate. The Voronoi pattern facilitated a more efficient distribution of material, enhancing the mechanical properties of the plate, such as stiffness, energy absorption, and fracture resistance under complex loading conditions, as confirmed in previous literature [68,71]. Voronoi tessellation was employed to optimize material distribution. The diameter of the cells was chosen considering both mechanical requirements and the printability of the reconstruction plate. Fig. 5 illustrates the algorithm used in the designing of the Voronoi plate. The algorithm utilized the data provided by the finite element analysis (FEA) to determine the optimal distribution of attractor points. Based on the FEA results, which highlighted areas of high and low stress, the algorithm adjusted the number of attractor points required in each region. In high-stress areas, the algorithm placed more attractor points to create a denser Voronoi pattern, enhancing structural support. Conversely, in low-stress areas, it reduced the number of points, resulting in larger cells and a more lightweight structure. This method allowed for an efficient distribution of material, ensuring strength where needed while minimizing unnecessary mass. This approach allows the design to be customized according to the specific anatomical needs of the patient.

The irregular cellular structure created by the Voronoi pattern helped achieve a more uniform stress distribution across the plate, reducing localized stress concentrations. This design strategy was used to enhance the mechanical performance of the plate, leading to potential improvements in stiffness, energy absorption, and the ability to handle complex, multi-directional forces. The arrangement of Voronoi cells, guided by attractor points, was specifically tailored to ensure the structure remained stable and mechanically strong while minimizing the overall mass of the plate.

By utilizing Voronoi tessellation on topology optimization, this method aimed to balance material efficiency and mechanical performance, reinforcing load-bearing regions and reducing material where it was not structurally necessary.

The latest models of reconstruction plates were subsequently imported into ANSYS (ANSYS Inc., USA) along with a more detailed mandible model that segmented separated cortical and trabecular bone for thorough scrutiny of the ultimate design performance. The latter analyses showed that both designs could withstand the masticatory forces.

Variables:

AP : Number of Voronoi attractor points
D : Diameter of the plate (mm)
$D_{min} = 1.5$ mm : Minimum diameter
$D_{max} = 2.5$ mm : Maximum diameter
$D_{base} = 2.0$ mm : Base diameter
$G_{min} = 1$ mm : Minimum Voronoi cell gap
LF_{base} : Base lightweight factor
$LF_{penalty\_point}$: Lightweight penalty per attractor point
$LF_{penalty\_diameter}$: Lightweight penalty per mm diameter increase
EF_{base} : Base endurance factor
$EF_{penalty\_diameter}$: Endurance penalty per mm diameter decrease

Formulas:
Lightweight Factor (LF):

$$LF = LF_{base} - (AP \times LF_{penalty\_point}) - ((D - D_{base}) \times LF_{penalty\_diameter})$$

Endurance Factor (EF):

$$EF = \begin{cases} EF_{base} - ((D_{base} - D) \times EF_{penalty\_diameter}) & \text{if } D < D_{base} \\ EF_{base} & \text{if } D \geq D_{base} \end{cases}$$

Combined Score (S):

$$S = LF + EF$$

Balanced Diameter:

$$D_{balanced} = \arg \max_{D \in [1.5, 2.5]} (S)$$

Key Points:

- Increasing AP makes lightweighting difficult.
- Larger D increases lightweight penalty, but $D < 2.0$ mm reduces endurance.
- Maintain $G_{min} = 1$ mm for Voronoi cells.

Fig. 5. The algorithms used to determine the cell dimension and plate thickness when performing topology optimization using the Voronoi pattern.

2.5. Designing and manufacturing the scaffold

In this study, a 0/90 porous hybrid scaffold was specifically designed for the defect site. An open-source slicing software was used for slicing. (Ultimaker CURA 4.6.1) Fig. 14 illustrates the design. The chosen materials were a commercially available blend of Tricalcium phosphate (TCP) and Polycaprolactone (PCL), which were further strengthened with an Hyaluronic acid dip coating (Bioscaffold Bloocell®). Tricalcium phosphate was selected as the inorganic matrix due to its osteoconductive properties, while Polycaprolactone is a well-established and approved material for various biomedical applications [72,73]. Extensive research has been conducted on combining these materials with PCL-TCP scaffolds, proving to be more efficient than using them individually [74]. The scaffolds demonstrate remarkable biocompatibility, which is manifested in favorable rates of cellular proliferation and adhesion [72]. Additionally, their biodegradability makes them ideal for controlled drug delivery applications, as demonstrated in previous literature [74–76]. The potential to load anti-cancer drugs onto these scaffolds to prevent recurrent cancers makes this material combination clinically significant [75]. It is also worth noting that hyaluronic acid plays a significant part in promoting the scaffold's mechanical properties, osteogenic effects, and degradation control [77–80]. The scaffold material used in this study has shown promising outcomes in clinical cases in maxillofacial and orthopedic surgery, including long bone fractures and guided bone regeneration [81,82]. A commercially available 3D bioprinter (Bloocell®) was used to print the scaffold. Fig. 15 depicts the printed scaffold. The diameter of the nozzle was tuned to 2 mm while adjusting the pore size to 400 μm to attain a pore size that is satisfactory for vascularization and mineral deposition while ensuring that the mechanical strength and cell viability are not compromised [83–85]. Following the printing and Hyaluronic acid dipping processes, the scaffold was subjected to an examination under a 40X zoom microscope. (Fig. 16) The visual representation in Fig. 17 showcases the integrated defect reconstruction plate and scaffold. The flowchart given below depicts an overall view of the entire process.(Fig. 18)

3. Results and discussion

This study investigated the management of segmental mandibular defects from a broad perspective. We designed patient-specific reconstruction plates to improve the reconstruction process and refined

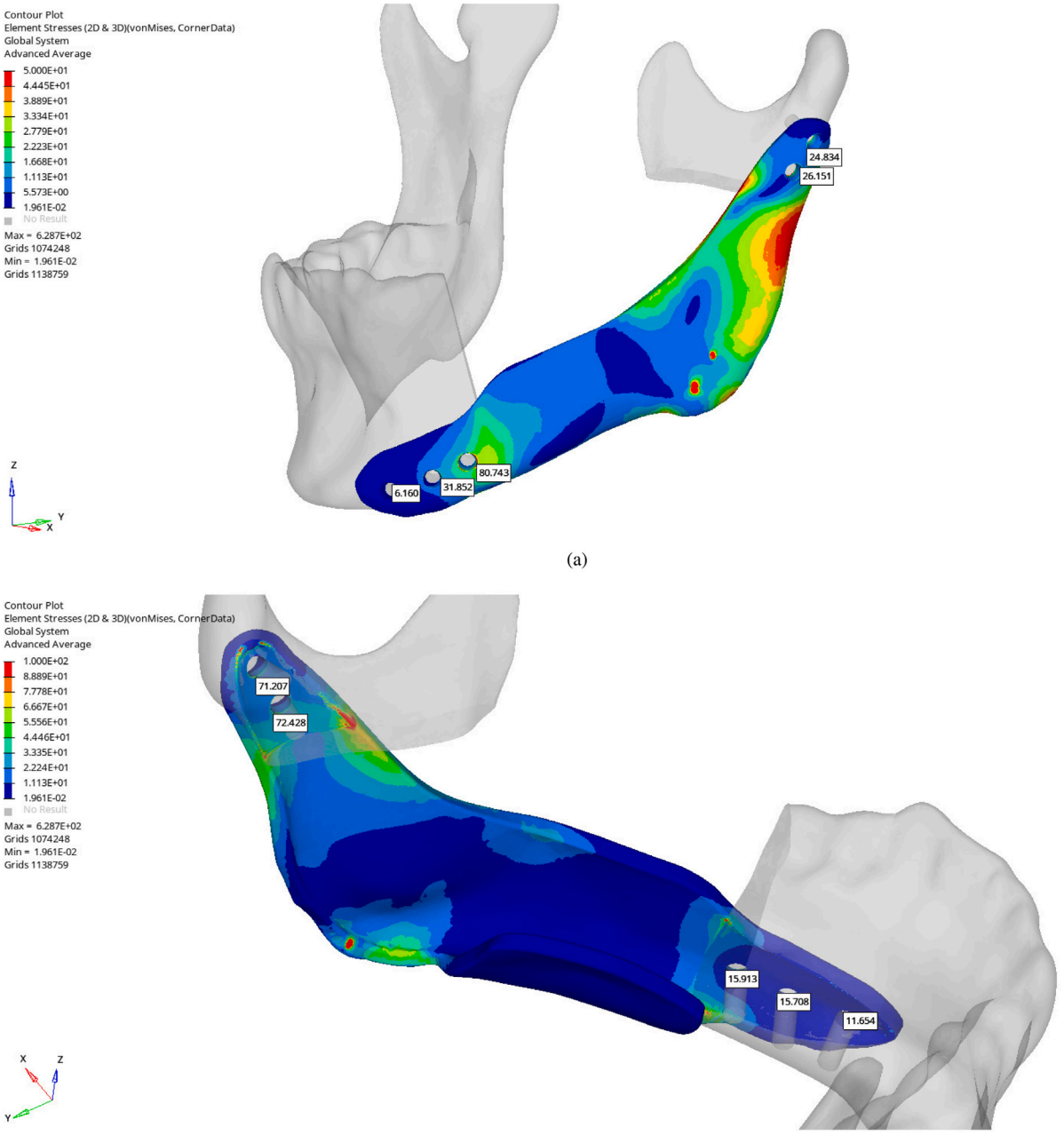

Fig. 6. Results of the first FEA with constrained right molars (a, b). Details of the analysis can be found in the Support Data.

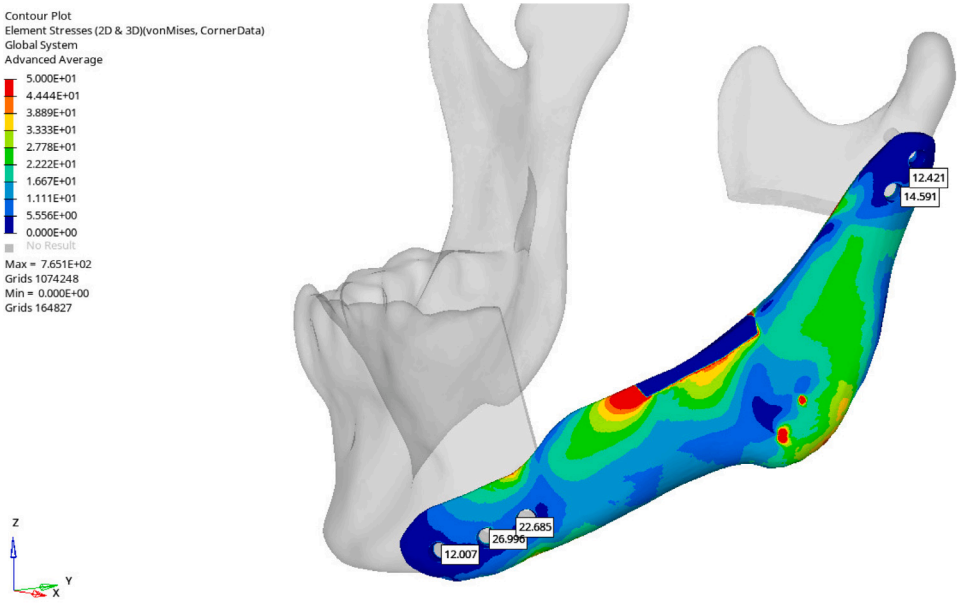

(a)

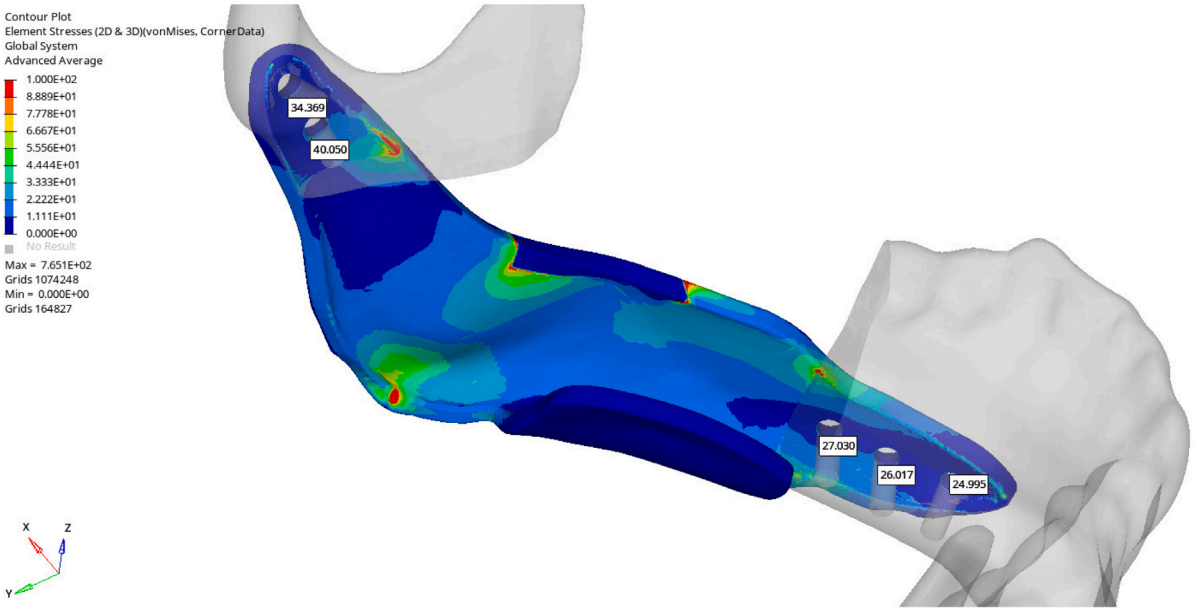

(b)

Fig. 7. Results of the first FEA with constrained left molars (c, d) Details of the analysis can be found in the Support Data.

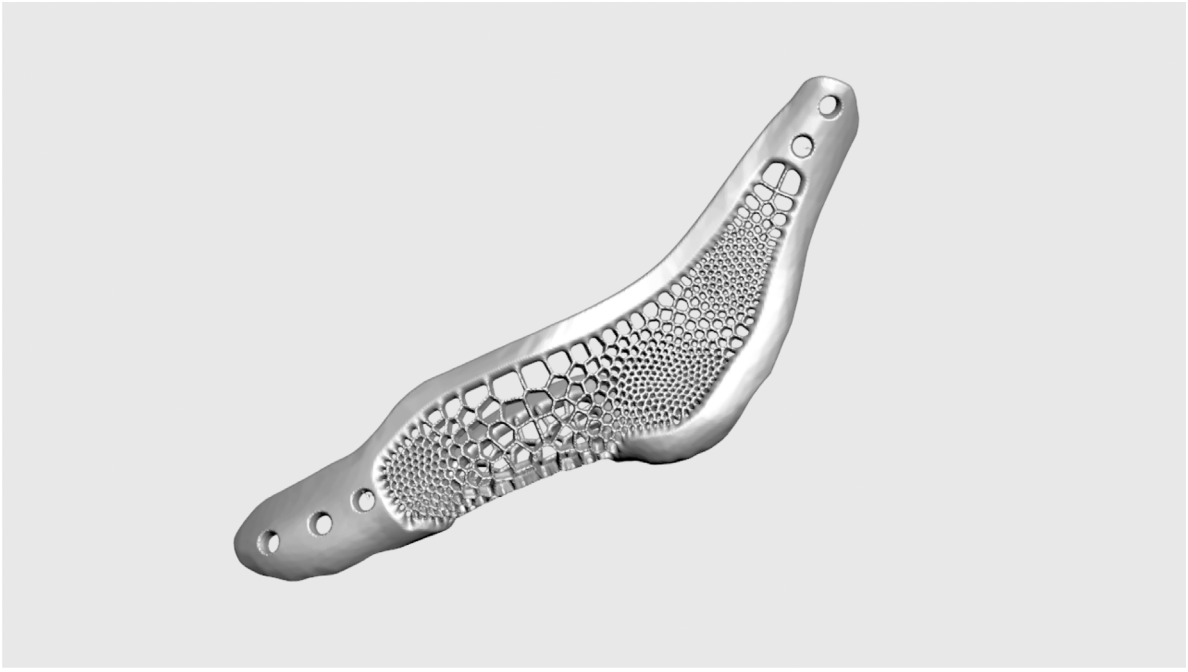

(a)

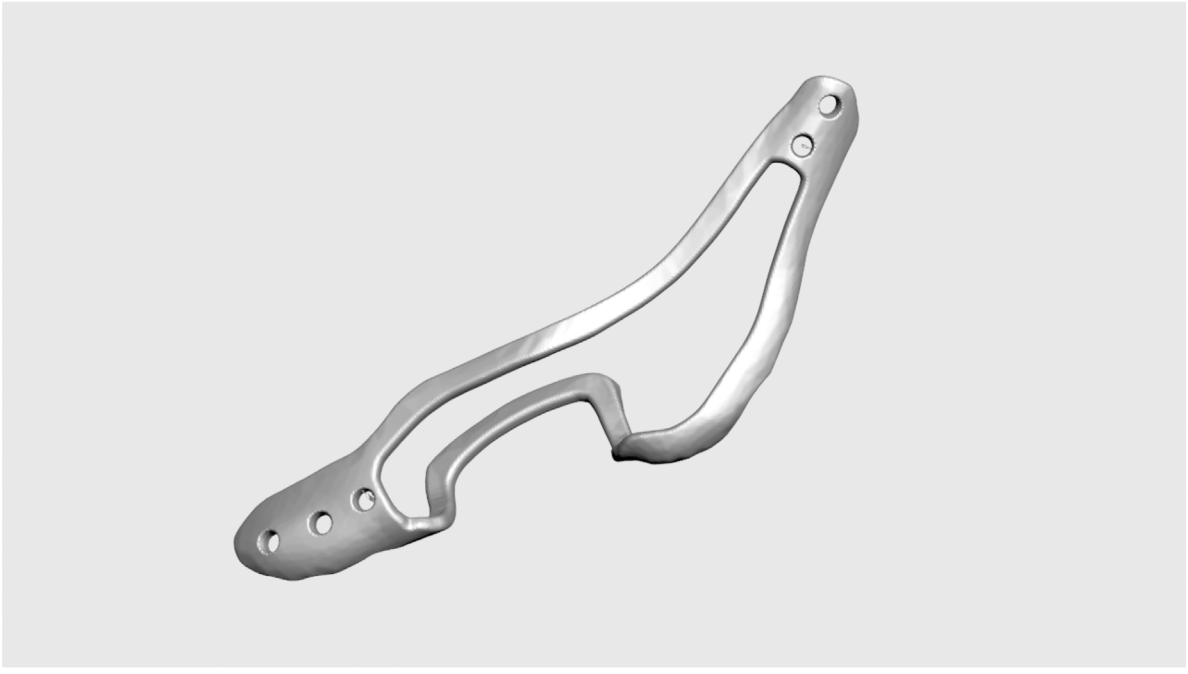

(b)

Fig. 8. The image shows the new reconstruction plate designs after topology optimization and light-weighting. (a)Voronoi Plate (b)Hollowed Plate.

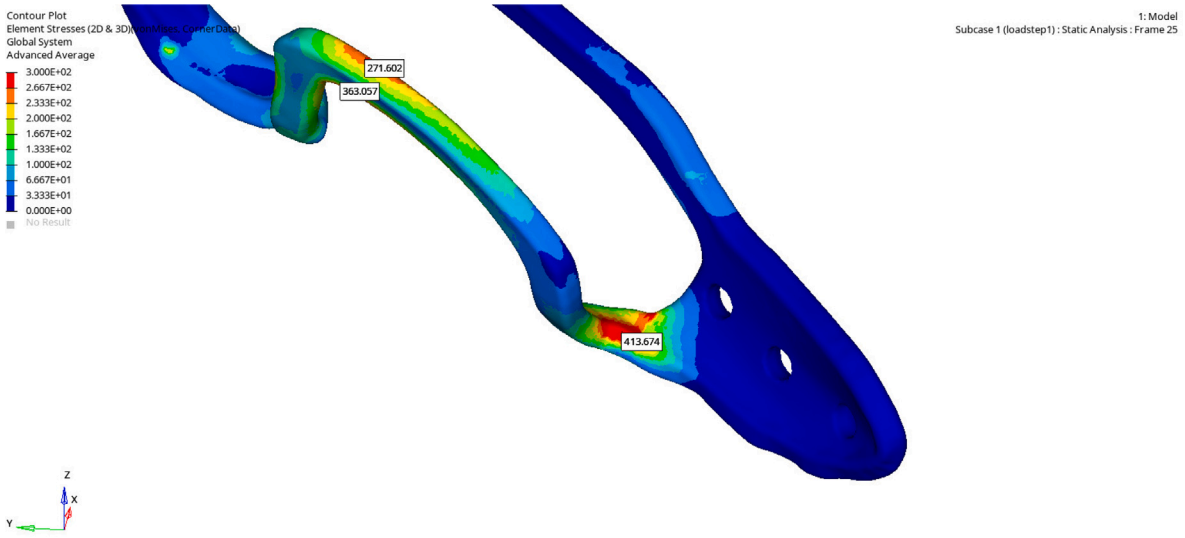

(a)

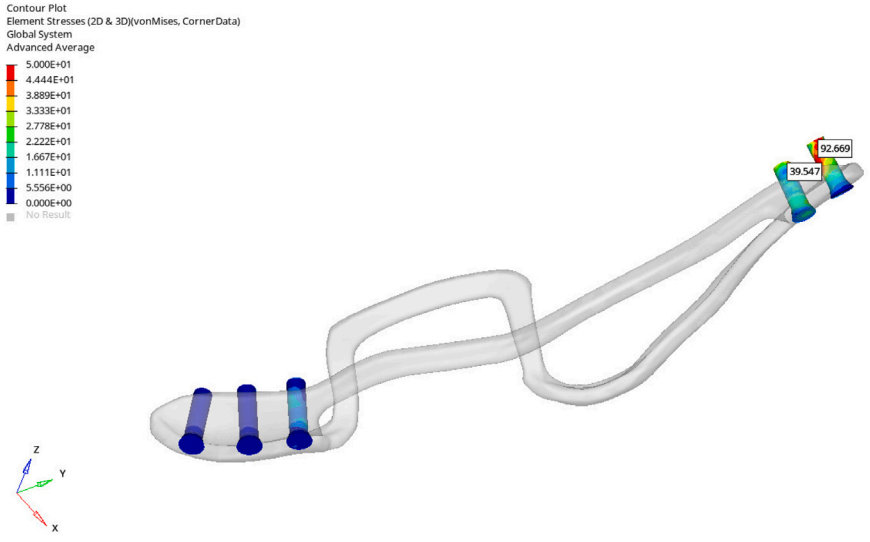

(b)

Fig. 9. Result of the static structural analysis of hollowed design with left molar constraint (a, b). Details of the analysis can be found in Support Data.

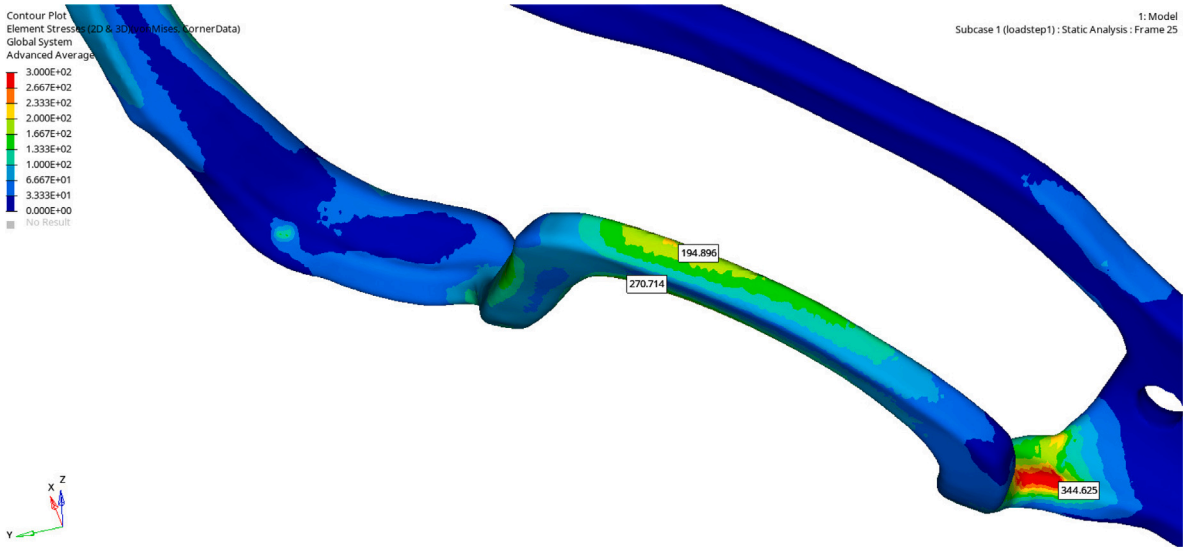

(a)

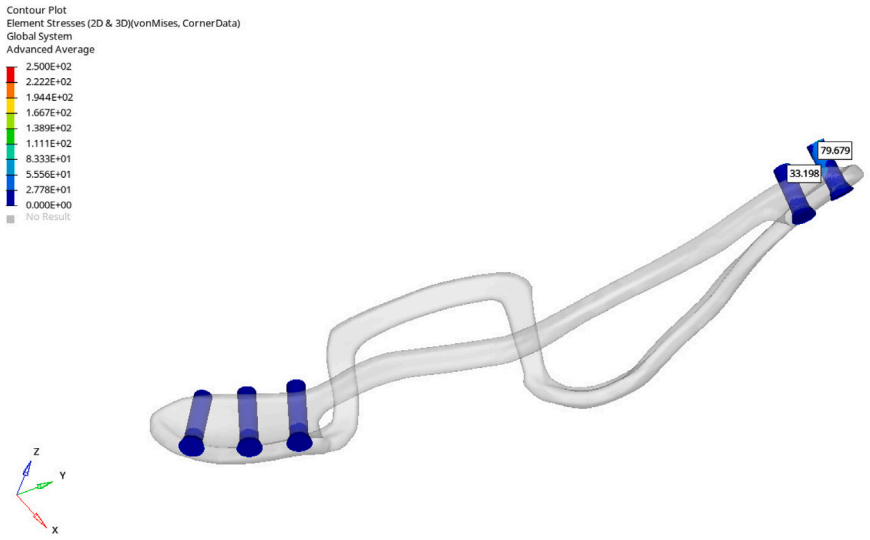

(b)

Fig. 10. Result of the static structural analysis of hollowed design with right molar constraint (c, d). Details of the analysis can be found in Support Data.

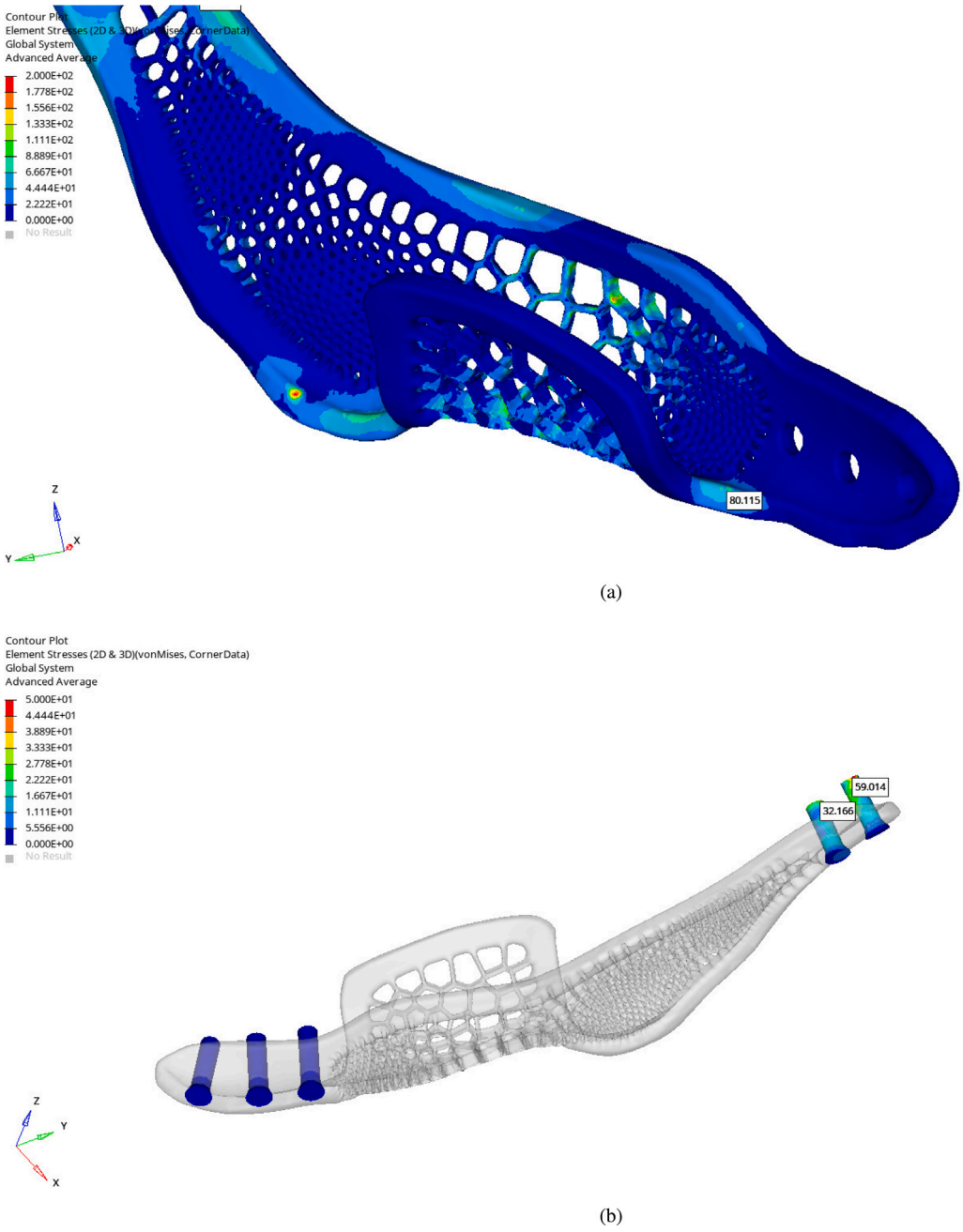

Fig. 11. Result of the static structural analysis of Voronoi plate with left molar constraint (a, b).

them through finite elemental analyses. The static structural analysis showed that during clenching of the left molars, the area of highest stress was located on the lingual side within the hollow design, while the titanium screw positioned at the condylar region experienced the greatest amount of stress, despite being far from the defect. Similarly, clenching with the right molars resulted in the base region of the mandible experiencing the highest stress. It should be noted that the maximum stress did not exceed the material's limits, indicating its potential for clinical application (Figs. 9, 10, Support Data). Overall, the analysis provides valuable insights into the stress distribution during molar clenching and the potential implications for implant design and placement.

The Voronoi tessellated plate demonstrated a notably homogeneous stress distribution, with maximum stress values remaining well within the material's capacity during both clenching tasks. The titanium screws exhibited outcomes that were comparable to those of the hollowed plate. These findings suggest that the Voronoi plate may be a viable option for withstanding diverse clinical scenarios. Figs. 11 and 12, and Support data show the analysis results.

Our research findings suggest that the Voronoi tessellation method has the potential to be an effective tool in designing anisotropic mandibular reconstruction plates. It is worth noting that there is no standard value for the mass of the human mandible, and previous studies have reported a range of 90.85 g ±16.08 for wet mandible mass [86]. By applying this range, we calculated the mass of our defect to be 20.3 g ±3.6. Initially, our reconstruction plate weighed 32.19 g, but after implementing topology optimization and lightweighting techniques, the Voronoi design weighed 20.21 g, and the hollowed design weighed 14.37 g. These results demonstrate that the Voronoi and hollowed designs provided a mass loss of % 37 and %

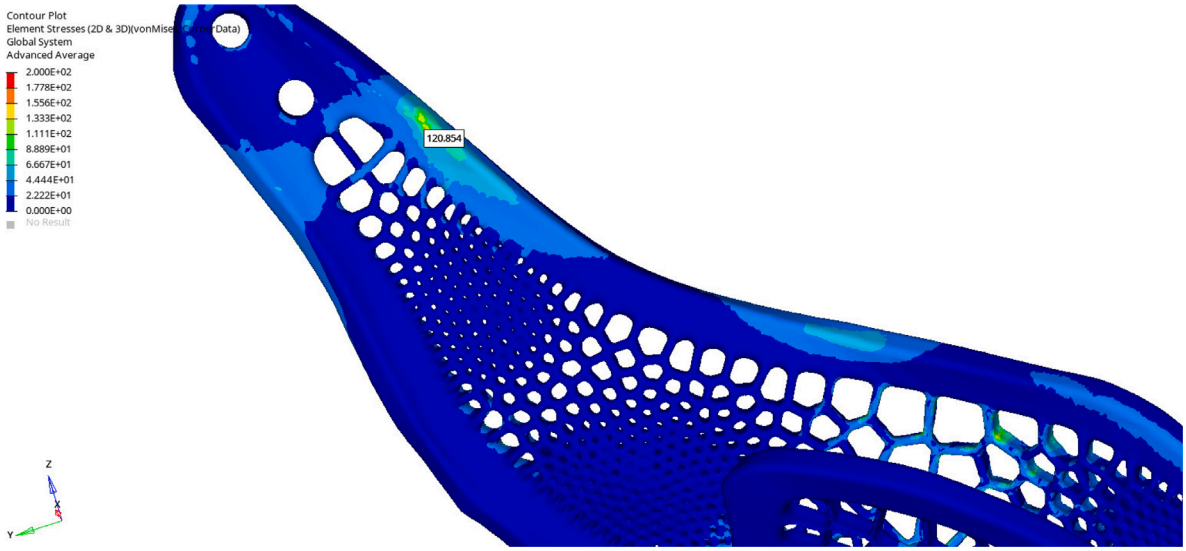

(a)

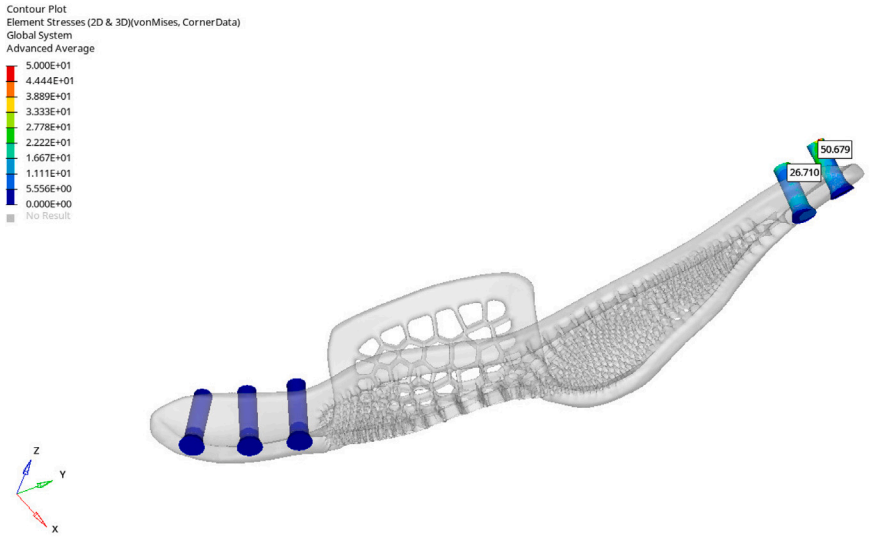

(b)

Fig. 12. Result of the static structural analysis of Voronoi plate with right molar constraint (c, d) Details of the analysis can be found in Support Data.

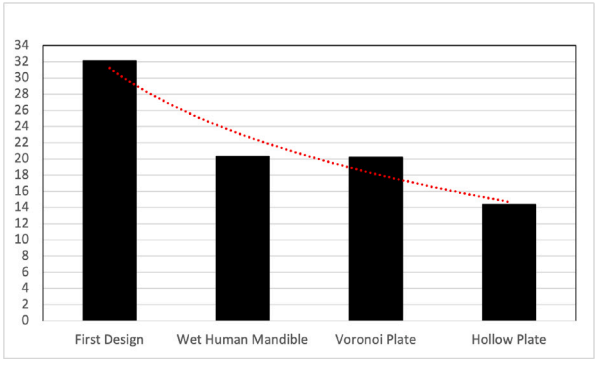

Fig. 13. The chart compares the weights of the native mandible and designed scaffolds.

55.34, respectively, approaching the weight of the original mandible(Table 4, Fig. 13) (see Fig. 8).

Table 4
The weights of the native mandible and designed reconstruction plates.

	Weight (grams)	Lightweighting (%)
First Designed Plate	32,1893556	x
Wet Human Mandible	20,3	x
Voronoi Plate	20,210304	37,2143254
Hollow Plate	14,3742504	55,3447091

To enhance the quality of future research, we need further studies to develop more advanced study models that accurately reflect the complex three-dimensional structure of the mandible and consider biological factors. We also need to conduct additional mechanical testing of the plates because current testing systems have limitations. These limitations include simplified test setups, lack of standardization, and an inability to fully capture the intricacies of the mandible's biomechanics. Therefore, it is essential to develop more sophisticated testing methods to overcome these limitations and provide more accurate and reliable results [16,30,56,87].

In this study, we used a TCP-PCL hybrid scaffold, augmented with Hyaluronic acid dipping, to improve the healing process by leveraging

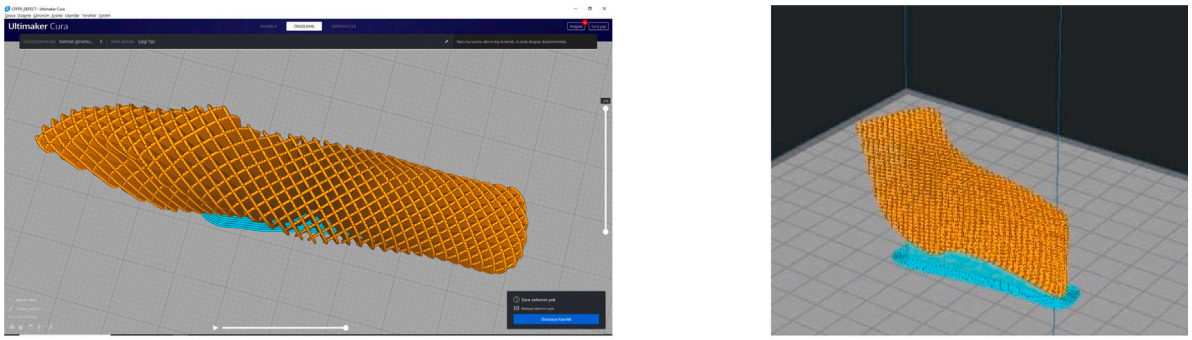

(a) (b)

Fig. 14. Design process of the scaffold.

(a) (b)

Fig. 15. Printed scaffold with support structure (a), after removing the support structure(b).

both organic and inorganic components. This approach holds significant promise for promoting tissue regeneration and improving patient outcomes. The scaffold has previously been used in clinical studies and performed well [81,82]. We have designed the scaffold to be used in segmental defects for the first time. Therefore, further animal experiments and clinical studies should be performed.

To manage the bone regeneration issue, it is crucial to conduct material selection and characterization and in-vitro studies of scaffolds. This is because none of the currently developed graft or scaffold systems have been able to fully replicate native bone tissue. Additionally, several areas require improvement, such as the formation of complex-structured scaffolds, duration of cell viability, efficacy of cell seeding, poor mechanical properties, biocompatibility issues, design challenges, and pore sizes and shapes [87–91].

Before the clinical implementation of our plate designs and hybrid scaffold system, it is essential to conduct animal studies after in-vitro testing to evaluate the overall efficacy of the components.

Modulating the pore size in accordance with the specific region could potentially imbue the scaffold with a biomimetic quality. Within the range of 200-900 μm, larger pore sizes have been observed to exhibit a positive correlation with increased calcification and vascularization, thereby targeting the cortical bone region, while smaller pore sizes micrometers are more suitable for the trabecular bone region [92,93].

As such, it is worth noting that despite the significant progress made in tissue engineering, free tissue flaps continue to be regarded as the gold standard for managing large segmental defects. Recently, bioprinting bioactive scaffolds has emerged as a promising strategy for addressing this issue. However, it is important to acknowledge that managing critical-size bone defects is a complex challenge, and as such, future solutions will likely require a multidisciplinary approach.

4. Conclusion

The present study delineates a comprehensive approach to managing segmental defects by utilizing novel mirroring parameters hitherto unused in virtual mandibular reconstruction. The said parameters might be beneficial exerting a favorable influence on anatomical and craniometric landmarks, thereby enhancing the precision and accuracy of the reconstruction process. The mandibular structure was carefully segmented, with trabecular and cortical bone separately, to allow for more precise simulation of clenching tasks and to enable a more defined stress distribution.

Two different clinical scenarios were considered in this study, and optimization was achieved for both scenarios through the design of two distinct plates: the hallowed plate, which is employed for long-term screening of recurrent cancer cases, and the Voronoi plate, which is intended for heavier load tasks when reconstruction with an autologous graft is not available. The hallowed plate can be removed after healing and is less burdensome than the original defect, so it could be used in combination with an autologous graft or a hybrid scaffold without causing any additional weight on the affected surgical area. The Voronoi plate is tailored to integrate with the bone and serve as a long-term solution. Its weight is comparable to the original defect, thereby minimizing any excessive weight on the surgical area.

Furthermore, the study involved the development of a hybrid TCP-PCL scaffold that was enhanced with Hyaluronic acid dipping to facilitate better healing. The scaffold was engineered to possess a tailored pore size that would enable suitable vascularization and bone formation. Before proceeding to the next stages, mechanical tests should be performed. In-vivo and animal studies should be conducted, followed

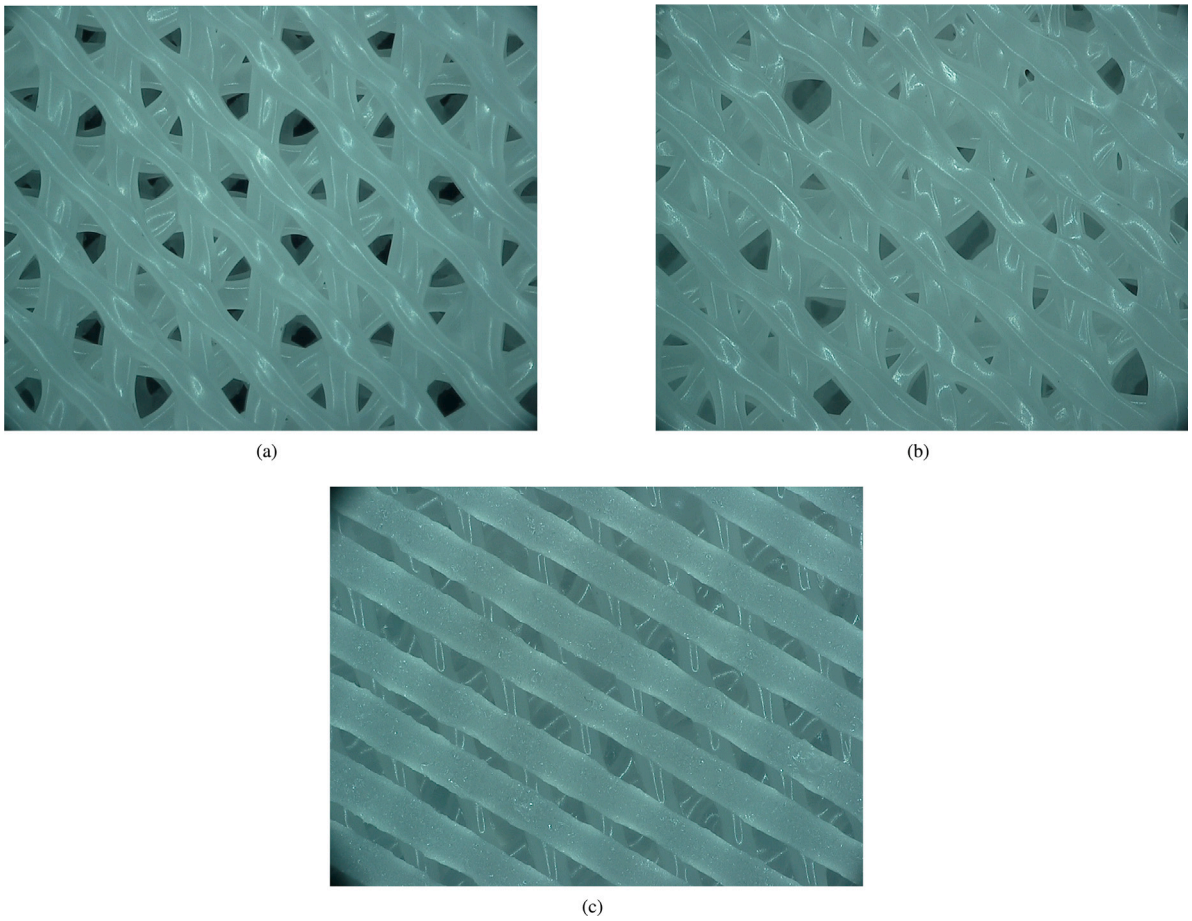

Fig. 16. The TCP-PCL scaffold inspected under the 40x zoom microscope. Before (a,b), and after(c) Hyaluronic Acid dipping.

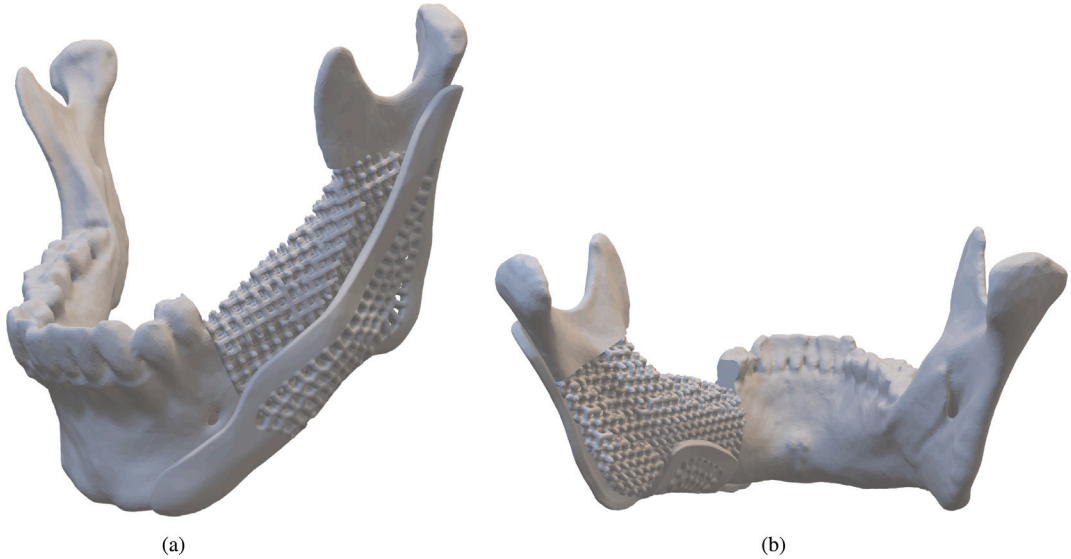

Fig. 17. The integrated image of the defect, Voronoi Plate, and the scaffold. The plate and the scaffold mimic the native tissue.

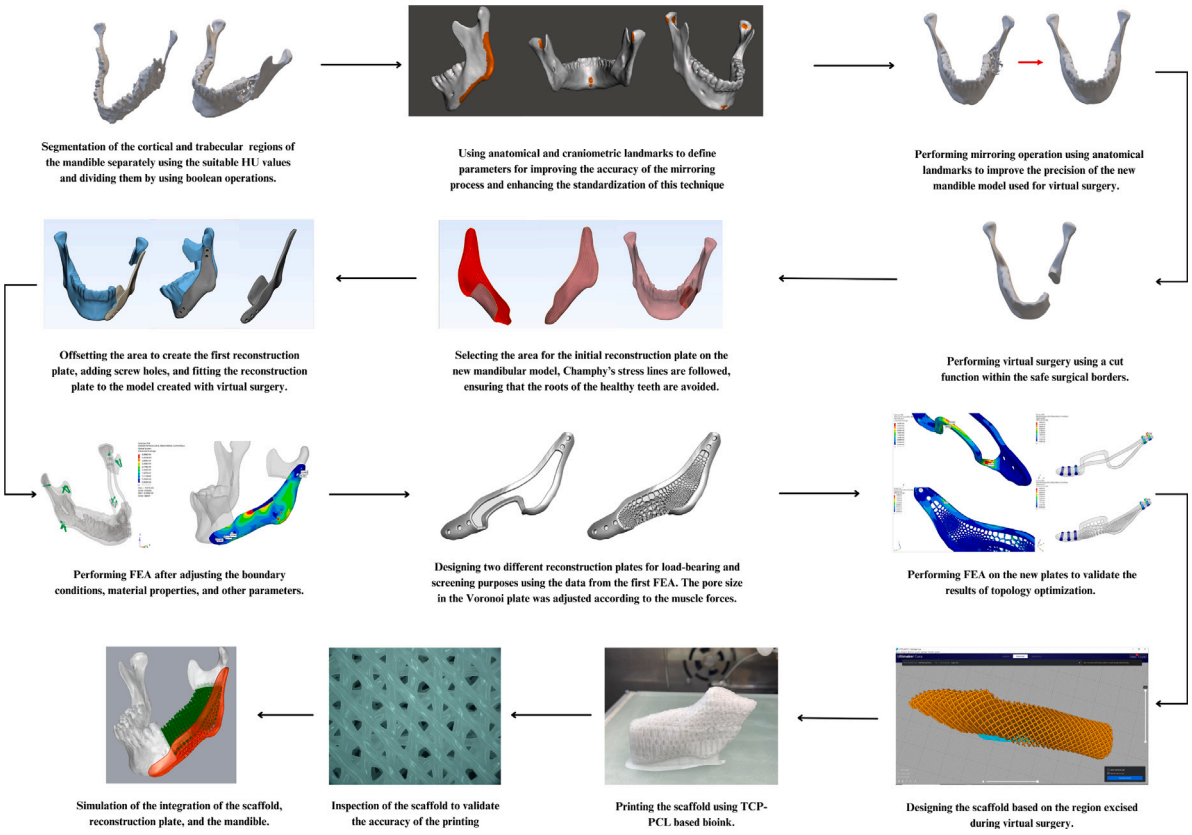

Fig. 18. A flowchart depicts the entire design process of the novel hybrid scaffold system.

by clinical studies that would help assess the performance of the reconstruction plates and the hybrid scaffold.

CRediT authorship contribution statement

Sait Emre Dogan: Writing – review & editing, Writing – original draft, Visualization, Validation, Supervision, Software, Resources, Project administration, Methodology, Investigation, Formal analysis, Data curation, Conceptualization. **Cengizhan Ozturk:** Validation, Supervision, Conceptualization. **Bahattin Koc:** Validation, Supervision, Methodology, Conceptualization.

Informed consent

Informed consent was obtained from the patient included in the study.

Declaration of competing interest

The authors declare that they have no known competing financial interests or personal relationships that could have appeared to influence the work reported in this article.

Appendix A. Supplementary data

Supplementary material related to this article can be found online at https://doi.org/10.1016/j.compbiomed.2024.109380.

References

[1] A.-M. Wu, C. Bisignano, S.L. James, G.G. Abady, A. Abedi, E. Abu-Gharbieh, R.K. Alhassan, V. Alipour, J. Arabloo, M. Asaad, W.N. Asmare, A.F. Awedew, M. Banach, S.K. Banerjee, A. Bijani, T.T.M. Birhanu, S.R. Bolla, L.A. Cámera, J.-C. Chang, D.Y. Cho, M.T. Chung, R.A.S. Couto, X. Dai, L. Dandona, R. Dandona, F. Farzadfar, I. Filip, F. Fischer, A.A. Fomenkov, T.K. Gill, B. Gupta, J.A. Haagsma, A. Haj-Mirzaian, S. Hamidi, S.I. Hay, I.M. Ilic, M.D. Ilic, R.Q. Ivers, M. Jürisson, R. Kalhor, T. Kanchan, T. Kavetskyy, R. Khalilov, E.A. Khan, M. Khan, C.J. Kneib, V. Krishnamoorthy, G.A. Kumar, N. Kumar, R. Lalloo, S. Lasrado, S.S. Lim, Z. Liu, A. Manafi, N. Manafi, R.G. Menezes, T.J. Meretoja, B. Miazgowski, T.R. Miller, Y. Mohammad, A. Mohammadian-Hafshejani, A.H. Mokdad, C.J.L. Murray, M. Naderi, M.D. Naimzada, V.C. Nayak, C.T. Nguyen, R. Nikbakhsh, A.T. Olagunju, N. Otstavnov, S.S. Otstavnov, J.R. Padubidri, J. Pereira, H.Q. Pham, M. Pinheiro, S. Polinder, H. Pourchamani, N. Rabiee, A. Radfar, M.H.U. Rahman, D.L. Rawaf, S. Rawaf, M.R. Saeb, A.M. Samy, L.S. Riera, D.C. Schwebel, S. Shahabi, M.A. Shaikh, A. Soheili, R. Tabarés-Seisdedos, M.R. Tovani-Palone, B.X. Tran, R.S. Travillian, P.R. Valdez, T.J. Vasankari, D.Z. Velazquez, N. Venketasubramanian, G.T. Vu, Z.-J. Zhang, T. Vos, Global, regional, and national burden of bone fractures in 204 countries and territories, 1990–2019: a systematic analysis from the Global Burden of Disease Study 2019, Lancet Healthy Longevity 2 (9) (2021) e580–e592, http://dx.doi.org/10.1016/s2666-7568(21)00172-0.
[2] T.A. Guise, Bone loss and fracture risk associated with cancer therapy, Oncologist 11 (10) (2006) 1121–1131, http://dx.doi.org/10.1634/theoncologist.11-10-1121.
[3] M.T. Drake, Osteoporosis and cancer, Curr. Osteoporos. Rep. 11 (3) (2013) 163–170, http://dx.doi.org/10.1007/s11914-013-0154-3.
[4] Z. Aversa, P. Costelli, M. Muscaritoli, Cancer-induced muscle wasting: latest findings in prevention and treatment, Therapeutic Adv. Med. Oncol. 9 (5) (2017) 369–382, http://dx.doi.org/10.1177/1758834017698643.
[5] M. Kheirallah, H. Almeshaly, Present strategies for critical bone defects regeneration, Oral Health Case Rep. 02 (03) (2016) http://dx.doi.org/10.4172/2471-8726.1000127.
[6] L. Vidal, C. Kampleitner, M.Á. Brennan, A. Hoornaert, P. Layrolle, Reconstruction of large skeletal defects: Current clinical therapeutic strategies and future directions using 3D printing, Front. Bioeng. Biotechnol. 8 (2020) http://dx.doi.org/10.3389/fbioe.2020.00061.
[7] E.M. Ferneini, M.T. Goupil, S. Halepas (Eds.), The History of Maxillofacial Surgery, Springer International Publishing, 2022, http://dx.doi.org/10.1007/978-3-030-89563-1.

[8] R. Schmoker, B. Spiessl, R. Mathys, A total mandibular plate to bridge large defects of the mandible, in: New Concepts in Maxillofacial Bone Surgery, Springer Berlin Heidelberg, 1976, pp. 156–159, http://dx.doi.org/10.1007/978-3-642-66484-7_22.

[9] A.S. Mao, D.J. Mooney, Regenerative medicine: Current therapies and future directions, Proc. Natl. Acad. Sci. 112 (47) (2015) 14452–14459, http://dx.doi.org/10.1073/pnas.1508520112.

[10] R. Langer, J.P. Vacanti, Tissue engineering, Science 260 (5110) (1993) 920–926, http://dx.doi.org/10.1126/science.8493529.

[11] J.P. Merrill, Successful homotransplantation of the human kidney between identical twins, JAMA 160 (4) (1956) 277, http://dx.doi.org/10.1001/jama.1956.02960390027008.

[12] K. Spencer, A. Sizeland, G. Taylor, D. Wiesenfeld, The use of titanium mandibular reconstruction plates in patients with oral cancer, Int. J. Oral Maxillofac. Surg. 28 (4) (1999) 288–290, http://dx.doi.org/10.1016/s0901-5027(99)80160-x.

[13] A. Sidambe, Biocompatibility of advanced manufactured titanium implants–a review, Materials (2014) http://dx.doi.org/10.3390/ma7128168.

[14] A.A. Almansoori, H.-W. Choung, B. Kim, J.-Y. Park, S.-M. Kim, J.-H. Lee, Fracture of standard titanium mandibular reconstruction plates and preliminary study of three-dimensional printed reconstruction plates, J. Oral. Maxillofac. Surg. (2020) http://dx.doi.org/10.1016/j.joms.2019.07.016.

[15] S. Maietta, A. Gloria, G. Improta, M. Richetta, R.D. Santis, M. Martorelli, A further analysis on Ti6Al4V lattice structures manufactured by selective laser melting, J. Healthc. Eng. (2019) http://dx.doi.org/10.1155/2019/3212594.

[16] D.C. Koper, C.A. Leung, L.C. Smeets, P.F. Laeven, G. Tuijthof, P.A. Kessler, Topology optimization of a mandibular reconstruction plate and biomechanical validation, J. Mech. Behav. Biomed. Mater. (2021) http://dx.doi.org/10.1016/j.jmbbm.2020.104157.

[17] L. Zhang, L. Chen, A review on biomedical titanium alloys: Recent progress and prospect, Adv. Eng. Mater. (2019) http://dx.doi.org/10.1002/adem.201801215.

[18] H. Rotaru, G. Armencea, D. Spîrchez, C. Berce, T. Marcu, D. Leordean, S.-G. Kim, S. Lee, C. Dinu, G. Băciuț, M. Baciut, In vivo behavior of surface modified Ti6Al7Nb alloys used in selective laser melting for custom-made implants. a preliminary study, Romanian J. Morphol. Embryol.=Revue Roumaine De Morphologie et Embryologie 54 (2013) 791–796.

[19] M. Sarraf, E.R. Ghomi, S. Alipour, S. Ramakrishna, N.L. Sukiman, A state-of-the-art review of the fabrication and characteristics of titanium and its alloys for biomedical applications, Bio-Des. Manuf. (2021) http://dx.doi.org/10.1007/s42242-021-00170-3.

[20] M. Niinomi, Index, Mater. Sci. Eng. A (1997) http://dx.doi.org/10.1016/s0921-5093(97)00469-3.

[21] S. Lampman, Titanium and its alloys for biomedical implants, Mater. Med. Dev. (2012) http://dx.doi.org/10.31399/asm.hb.v23.a0005674.

[22] K.E. Blackwell, V. Lacombe, The bridging lateral mandibular reconstruction plate revisited, Arch. Otolaryngol. Head Neck Surg. (1999) http://dx.doi.org/10.1001/archotol.125.9.988.

[23] J. Ferreira, C.M. Zagalo, M.L. Oliveira, A. Correia, A.R. Reis, Mandible reconstruction, Prosthet. Orthot. Int. (2015) http://dx.doi.org/10.1177/0309364613520032.

[24] B.P. Kumar, V. Venkatesh, K.A.J. Kumar, B.Y. Yadav, S.R. Mohan, Mandibular reconstruction: Overview, J. Maxillofac. Oral Surg. (2015) http://dx.doi.org/10.1007/s12663-015-0766-5.

[25] B.W. Burger, Primary mandibular reconstruction using the AO reconstruction plate, J. Oral. Maxillofac. Surg. (1987) http://dx.doi.org/10.1016/0278-2391(87)90101-7.

[26] G.-J. Seol, E.-G. Jeon, J.-S. Lee, S.-Y. Choi, J.-W. Kim, T.-G. Kwon, J.-Y. Paeng, Reconstruction plates used in the surgery for mandibular discontinuity defect, J. Korean Assoc. Oral Maxillofac. Surgeons (2014) http://dx.doi.org/10.5125/jkaoms.2014.40.6.266.

[27] D.W. Klotch, T.J. Gal, R.L. Gal, Assessment of plate use for mandibular reconstruction: Has changing technology made a difference? Otol. Head Neck Surg. (1999) http://dx.doi.org/10.1016/s0194-5998(99)70226-3.

[28] A. Al-Ahmari, E.A. Nasr, K. Moiduddin, S. Anwar, M.A. Kindi, A. Kamrani, A comparative study on the customized design of mandibular reconstruction plates using finite element method, Adv. Mech. Eng. (2015) http://dx.doi.org/10.1177/1687814015593890.

[29] A. Katakura, T. Shibahara, H. Noma, M. Yoshinari, Material analysis of AO plate fracture cases, J. Oral. Maxillofac. Surg. (2004) http://dx.doi.org/10.1016/j.joms.2003.05.009.

[30] S.-M. Park, S. Park, J. Park, M. Choi, L. Kim, G. Noh, Design process of patient-specific osteosynthesis plates using topology optimization, J. Comput. Des. Eng. (2021) http://dx.doi.org/10.1093/jcde/qwab047.

[31] F. Wilde, H. Hanken, F. Probst, A. Schramm, M. Heiland, C.-P. Cornelius, Multicenter study on the use of patient-specific CAD/CAM reconstruction plates for mandibular reconstruction, Int. J. Comput. Assisted Radiol. Surg. (2015) http://dx.doi.org/10.1007/s11548-015-1193-2.

[32] C.-P. Cornelius, W. Smolka, G.A. Giessler, F. Wilde, F.A. Probst, Patient-specific reconstruction plates are the missing link in computer-assisted mandibular reconstruction: A showcase for technical description, J. Cranio-Maxillofac. Surg. (2015) http://dx.doi.org/10.1016/j.jcms.2015.02.016.

[33] L. Hijazi, W. Hejazi, M.A. Darwich, K. Darwich, Finite element analysis of stress distribution on the mandible and condylar fracture osteosynthesis during various clenching tasks, Oral Maxillofac. Surg. (2016) http://dx.doi.org/10.1007/s10006-016-0573-2.

[34] A. Dutta, K. Mukherjee, S. Dhara, S. Gupta, Design of porous titanium scaffold for complete mandibular reconstruction: The influence of pore architecture parameters, Comput. Biol. Med. (2019) http://dx.doi.org/10.1016/j.compbiomed.2019.03.004.

[35] J. Kang, J. Zhang, J. Zheng, L. Wang, D. Li, S. Liu, 3D-printed PEEK implant for mandibular defects repair - a new method, J. Mech. Behav. Biomed. Mater. (2021) http://dx.doi.org/10.1016/j.jmbbm.2021.104335.

[36] S. Kargarnejad, F. Ghalichi, M. Pourgol-Mohammad, A. Garajei, Mandibular reconstruction system reliability analysis using probabilistic finite element method, Comput. Methods Biomech. Biomed. Eng. (2021) http://dx.doi.org/10.1080/10255842.2021.1892660.

[37] I.T. Ozbolat, 3D Bioprinting, Elsevier, 2017, http://dx.doi.org/10.1016/c2014-0-02349-0.

[38] N.A. Sears, D.R. Seshadri, P.S. Dhavalikar, E. Cosgriff-Hernandez, A review of three-dimensional printing in tissue engineering, Tissue Eng. B: Rev. 22 (4) (2016) 298–310, http://dx.doi.org/10.1089/ten.teb.2015.0464.

[39] S. Mondal, U. Pal, 3D hydroxyapatite scaffold for bone regeneration and local drug delivery applications, J. Drug Deliv. Sci. Technol. (2019) http://dx.doi.org/10.1016/j.jddst.2019.101131.

[40] Y. Zha, Y. Li, T. Lin, J. Chen, S. Zhang, J. Wang, Progenitor cell-derived exosomes endowed with VEGF plasmids enhance osteogenic induction and vascular remodeling in large segmental bone defects, Theranostics (2021) http://dx.doi.org/10.7150/thno.50741.

[41] S.K. Wong, M.M.F. Yee, K.-Y. Chin, S. Ima-Nirwana, A review of the application of natural and synthetic scaffolds in bone regeneration, J. Funct. Biomater. (2023) http://dx.doi.org/10.3390/jfb14050286.

[42] S. Prasadh, R.C.W. Wong, Unraveling the mechanical strength of biomaterials used as a bone scaffold in oral and maxillofacial defects, Oral Sci. Int. (2018) http://dx.doi.org/10.1016/s1348-8643(18)30005-3.

[43] A. Tampieri, E. Landi, F. Valentini, M. Sandri, T. D'Alessandro, V. Dediu, M. Marcacci, A conceptually new type of bio-hybrid scaffold for bone regeneration, Nanotechnology (2010) http://dx.doi.org/10.1088/0957-4484/22/1/015104.

[44] D. Bhattarai, L. Aguilar, C. Park, C. Kim, A review on properties of natural and synthetic based electrospun fibrous materials for bone tissue engineering, Membranes (2018) http://dx.doi.org/10.3390/membranes8030062.

[45] F. Donnaloja, E. Jacchetti, M. Soncini, M.T. Raimondi, Natural and synthetic polymers for bone scaffolds optimization, Polymers (2020) http://dx.doi.org/10.3390/polym12040905.

[46] M. Filippi, G. Born, M. Chaaban, A. Scherberich, Natural polymeric scaffolds in bone regeneration, Front. Bioeng. Biotechnol. (2020) http://dx.doi.org/10.3389/fbioe.2020.00474.

[47] C. Gkioni, S. Leeuwenburgh, J. Jansen, Bone tissue engineering: Biodegradable polymeric–ceramic composite scaffolds for tissue regeneration, Encycl. Biomed. Polym. Polym. Biomater. (2016) http://dx.doi.org/10.1081/e-ebpp-120052254.

[48] S. Torgbo, P. Sukyai, Fabrication of microporous bacterial cellulose embedded with magnetite and hydroxyapatite nanocomposite scaffold for bone tissue engineering, Mater. Chem. Phys. (2019) http://dx.doi.org/10.1016/j.matchemphys.2019.121868.

[49] H.-W. Kim, J.C. Knowles, H.-E. Kim, Hydroxyapatite/poly(ϵ-caprolactone) composite coatings on hydroxyapatite porous bone scaffold for drug delivery, Biomaterials (2004) http://dx.doi.org/10.1016/j.biomaterials.2003.07.003.

[50] N. Amiryaghoubi, N.N. Pesyan, M. Fathi, Y. Omidi, Injectable thermosensitive hybrid hydrogel containing graphene oxide and chitosan as dental pulp stem cells scaffold for bone tissue engineering, Int. J. Biiol. Macromol. (2020) http://dx.doi.org/10.1016/j.ijbiomac.2020.06.138.

[51] S.S. Lee, M. Santschi, S.J. Ferguson, A biomimetic macroporous hybrid scaffold with sustained drug delivery for enhanced bone regeneration, Biomacromolecules (2021) http://dx.doi.org/10.1021/acs.biomac.1c00241.

[52] H. Shao, J. He, T. Lin, Z. Zhang, Y. Zhang, S. Liu, 3D gel-printing of hydroxyapatite scaffold for bone tissue engineering, Ceram. Int. (2019) http://dx.doi.org/10.1016/j.ceramint.2018.09.300.

[53] K. Maki, A. Miller, T. Okano, Y. Shibasaki, Changes in cortical bone mineralization in the developing mandible: A three–dimensional quantitative computed tomography study, J. Bone Miner. Res. (2000) http://dx.doi.org/10.1359/jbmr.2000.15.4.700.

[54] A. Tabassum, M.K.C. Singh, N. Ibrahim, S. Ramanarayanan, M.Y.P.M. Yusof, Quantifications of mandibular trabecular bone microstructure using cone beam computed tomography for age estimation: A preliminary study, Biology (2022) http://dx.doi.org/10.3390/biology11101521.

[55] C.E. Misch, Density of bone: effect on treatment plans, surgical approach, healing, and progressive boen loading, Int. J. Oral Implantol.: Implantol. 6 (2) (1990) 23–31.

[56] R. Wong, H. Tideman, L. Kin, M. Merkx, Biomechanics of mandibular reconstruction: a review, Int. J. Oral Maxillofac. Surg. (2010) http://dx.doi.org/10.1016/j.ijom.2009.11.003.

[57] J. Koshy, E. Feldman, C. Chike-Obi, J. Bullocks, Pearls of mandibular trauma management, Semin. Plastic Surg. (2010) http://dx.doi.org/10.1055/s-0030-1269765.
[58] G. Singh, B. Harjani, R. Singh, U. Pal, Locking v/s non-locking reconstruction plates in mandibular reconstruction, Natl. J. Maxillofac. Surg. (2012) http://dx.doi.org/10.4103/0975-5950.111371.
[59] Not available, Mechanical testing of bone and the bone-implant interface, 1999, http://dx.doi.org/10.1201/9781420073560, Not available.
[60] É. Lakatos, L. Magyar, I. Bojtár, Material properties of the mandibular trabecular bone, J. Med. Eng. (2014) http://dx.doi.org/10.1155/2014/470539.
[61] T.W. Korioth, A.G. Hannam, Mandibular forces during simulated tooth clenching, J. Oral Facial Pain Headache (1994) URL https://pubmed.ncbi.nlm.nih.gov/7920353/.
[62] F. Wilde, C.-P. Cornelius, A. Schramm, Computer-assisted mandibular reconstruction using a patient-specific reconstruction plate fabricated with computer-aided design and manufacturing techniques, Craniomaxillofac. Trauma Reconstr. (2014) http://dx.doi.org/10.1055/s-0034-1371356.
[63] A. Jahadakbar, N.S. Moghaddam, A. Amerinatanzi, D. Dean, H. Karaca, M. Elahinia, Finite element simulation and additive manufacturing of stiffness-matched NiTi fixation hardware for mandibular reconstruction surgery, Bioengineering (2016) http://dx.doi.org/10.3390/bioengineering3040036.
[64] P. Ruf, V. Orassi, H. Fischer, C. Steffen, G.N. Duda, M. Heiland, K. Kreutzer, S. Checa, C. Rendenbach, Towards mechanobiologically optimized mandible reconstruction: CAD/CAM miniplates vs. reconstruction plates for fibula free flap fixation: A finite element study, Front. Bioeng. Biotechnol. (2022) http://dx.doi.org/10.3389/fbioe.2022.1005022.
[65] Y. feng Liu, Y. ying Fan, X. feng Jiang, D.A. Baur, A customized fixation plate with novel structure designed by topological optimization for mandibular angle fracture based on finite element analysis, BioMed. Eng. OnLine (2017) http://dx.doi.org/10.1186/s12938-017-0422-z.
[66] F. Feng, S. Xiong, Z. Liu, Z. Xian, Y. Zhou, H. Kobayashi, A. Kawamoto, T. Nomura, B. Zhu, Cellular topology optimization on differentiable Voronoi diagrams, Internat. J. Numer. Methods Engrg. 124 (2022) 282–304, http://dx.doi.org/10.1002/nme.7121.
[67] D. Sieger, P. Alliez, M. Botsch, Optimizing voronoi diagrams for polygonal finite element computations, in: Proceedings of the 19th International Meshing Roundtable, Not available, Springer Berlin Heidelberg, 2010, pp. 335–350, http://dx.doi.org/10.1007/978-3-642-15414-0_20.
[68] J. Deering, K.I. Dowling, L.-A. DiCecco, G.D. McLean, B. Yu, K. Grandfield, Selective voronoi tessellation as a method to design anisotropic and biomimetic implants, J. Mech. Behav. Biomed. Mater. (2021) http://dx.doi.org/10.1016/j.jmbbm.2021.104361.
[69] N. Sharma, D. Ostas, H. Rotar, P. Brantner, F.M. Thieringer, Design and additive manufacturing of a biomimetic customized cranial implant based on voronoi diagram, Front. Physiol. (2021) http://dx.doi.org/10.3389/fphys.2021.647923.
[70] H. Zhao, Y. Han, C. Pan, D. Yang, H. Wang, T. Wang, X. Zeng, P. Su, Design and mechanical properties verification of gradient voronoi scaffold for bone tissue engineering, Micromachines (2021) http://dx.doi.org/10.3390/mi12060664.
[71] Z. Alknery, Z.D.I. Sktani, A. Arab, Effect of cell geometry on the mechanical properties of 3D voronoi tessellation, J. Funct. Biomater. 13 (2022) 302, http://dx.doi.org/10.3390/jfb13040302.
[72] W. Xue, A. Bandyopadhyay, S. Bose, Polycaprolactone coated porous tricalcium phosphate scaffolds for controlled release of protein for tissue engineering, J. Biomed. Mater. Res. B: Appl. Biomater. (2009) http://dx.doi.org/10.1002/jbm.b.31464.
[73] S.-H. Huang, T.-T. Hsu, T.-H. Huang, C.-Y. Lin, M.-Y. Shie, Fabrication and characterization of polycaprolactone and tricalcium phosphate composites for tissue engineering applications, J. Dental Sci. (2017) http://dx.doi.org/10.1016/j.jds.2016.05.003.
[74] S.A. Park, H.-J. Lee, S.-Y. Kim, K.-S. Kim, D.-W. Jo, S.-Y. Park, Three-dimensionally printed polycaprolactone/beta-tricalcium phosphate scaffold was more effective as an <scp>rhBMP</scp>-2 carrier for new bone formation than polycaprolactone alone, J. Biomed. Mater. Res. A (2020) http://dx.doi.org/10.1002/jbm.a.37075.
[75] G. Janarthanan, I.G. Kim, E.-J. Chung, I. Noh, Comparative studies on thin polycaprolactone-tricalcium phosphate composite scaffolds and its interaction with mesenchymal stem cells, Biomater. Res. (2019) http://dx.doi.org/10.1186/s40824-018-0153-7.
[76] C.-M. Chen, S.-M. Chen, S.-F. Lin, H.-C. Liang, C.-C. Wu, Clinical efficacy of polycaprolactone β-calcium triphosphate composite for osteoconduction in rabbit bone defect model, Polymers (2021) http://dx.doi.org/10.3390/polym13152552.
[77] J. Patterson, R. Siew, S.W. Herring, A.S. Lin, R. Guldberg, P.S. Stayton, Hyaluronic acid hydrogels with controlled degradation properties for oriented bone regeneration, Biomaterials 31 (2010) 6772–6781, http://dx.doi.org/10.1016/j.biomaterials.2010.05.047.
[78] A.C. Muran, B.C. Schaffler, A. Wong, E. Neufeld, P. Swami, M. Pianka, D. Grande, Effect of increasing hyaluronic acid content in collagen scaffolds on the maintenance of chondrogenic phenotype in chondrocytes and mesenchymal stem cells, J. Cartilage Joint Preserv. 3 (2023) 100099, http://dx.doi.org/10.1016/j.jcjp.2023.100099.
[79] P. Zhai, X. Peng, B. Li, Y. Liu, H. Sun, X. Li, The application of hyaluronic acid in bone regeneration, Int. J. Biiol. Macromol. 151 (2020) 1224–1239, http://dx.doi.org/10.1016/j.ijbiomac.2019.10.169.
[80] F. Xing, C. Zhou, D. Hui, C. Du, L. Wu, L. Wang, W. Wang, X. Pu, L. Gu, L. Liu, Z. Xiang, X. Zhang, Hyaluronic acid as a bioactive component for bone tissue regeneration: Fabrication, modification, properties, and biological functions, Nanotechnol. Rev. 9 (2020) 1059–1079, http://dx.doi.org/10.1515/ntrev-2020-0084.
[81] Not available, E-poster, Clin. Oral Implants Res. 34 (2023) 50–253, http://dx.doi.org/10.1111/clr.14162.
[82] E. Özdemir, F. Familiari, P.Y. Huri, A. Firat, G. Huri, Use of 3D-printed polycaprolactone + hyaluronic acid-based scaffold in orthopedic practice: Report of two cases, J. 3D Print. Med. 7 (2023) http://dx.doi.org/10.2217/3dp-2022-0020, Not available.
[83] Y. Xu, F. Zhang, W. Zhai, S. Cheng, J. Li, Y. Wang, Unraveling of advances in 3D-printed polymer-based bone scaffolds, Polymers (2022) http://dx.doi.org/10.3390/polym14030566.
[84] J. Lee, D. Kim, C.H. Jang, G.H. Kim, Highly elastic 3D-printed gelatin/HA/placental-extract scaffolds for bone tissue engineering, Theranostics (2022) http://dx.doi.org/10.7150/thno.73146.
[85] M. Bahraminasab, Challenges on optimization of 3D-printed bone scaffolds, BioMed. Eng. OnLine (2020) http://dx.doi.org/10.1186/s12938-020-00810-2.
[86] F. Zhang, C.C. Peck, A.G. Hannam, Mass properties of the human mandible, J. Biomech. (2002) http://dx.doi.org/10.1016/s0021-9290(02)00057-x.
[87] R. Gutwald, R. Jaeger, F.M. Lambers, Customized mandibular reconstruction plates improve mechanical performance in a mandibular reconstruction model, Comput. Methods Biomech. Biomed. Eng. (2016) http://dx.doi.org/10.1080/10255842.2016.1240788.
[88] M. Krishani, W.Y. Shin, H. Suhaimi, N.S. Sambudi, Development of scaffolds from bio-based natural materials for tissue regeneration applications: A review, Gels (2023) http://dx.doi.org/10.3390/gels9020100.
[89] B.P. Chan, K.W. Leong, Scaffolding in tissue engineering: general approaches and tissue-specific considerations, Eur. Spine J. (2008) http://dx.doi.org/10.1007/s00586-008-0745-3.
[90] L. Suamte, A. Tirkey, J. Barman, P.J. Babu, Various manufacturing methods and ideal properties of scaffolds for tissue engineering applications, Smart Mater. Manuf. (2023) http://dx.doi.org/10.1016/j.smmf.2022.100011.
[91] M. Wang, Materials selection and scaffold fabrication for tissue engineering in orthopaedics, in: Qin (Ed.), Advanced Bioimaging Technologies in Assessment of the Quality of Bone and Scaffold Materials: Techniques and Applications, Springer Berlin Heidelberg, Berlin, Heidelberg, 2007, pp. 259–288, http://dx.doi.org/10.1007/978-3-540-45456-4_16.
[92] N. Abbasi, S. Hamlet, R.M. Love, N.-T. Nguyen, Porous scaffolds for bone regeneration, J. Sci.: Adv. Mater. Dev. 5 (1) (2020) 1–9, http://dx.doi.org/10.1016/j.jsamd.2020.01.007, URL https://www.sciencedirect.com/science/article/pii/S2468217920300071.
[93] Y. Niu, L. Chen, T. Wu, Recent advances in bioengineering bone revascularization based on composite materials comprising hydroxyapatite, Int. J. Mol. Sci. (2023) http://dx.doi.org/10.3390/ijms241512492.

Sait Emre Doğan He joined the Ataturk University Faculty of Dentistry in 2013, then exchanged to the Necmettin Erbakan University Faculty of Dentistry. His studies were on orthognathic surgery. After graduating from Necmettin Erbakan University Faculty of Dentistry in 2019, he worked in private practice in different clinics in İzmir and Okan University Dental Hospital and Yildiz Technical University Community Health Center in Istanbul. From 2021 he joined the X-Lab in Bogazici University and conduct research on bioprinting, reconstruction of mandible and bone graft materials with Cengizhan Ozturk from Bogazici University and Bahattin Koc from SabancıUniversity. He is currently working as a dentist in Yildiz Technical University Community Health Center.

Cengihan Ozturk During 1997–2000, he worked as a postdoctoral research fellow at Medical Imaging Lab, Department of Biomedical Engineering, Johns Hopkins University. Between 1999–2000, he also worked at the Laboratory of Cardiac Energetics, National Heart Lung Blood Institute (NHLBI, NIH). His postgraduate work has always focused on various topics in Magnetic Resonance Imaging. He started to work at Bogazici University in 2000, later visited Cardiac Interventions Lab at NHLBI, NIH between 2003 and 2005 as a visiting scientist to work on MR guided medical interventions. He is currently working as a Professor at the Institute of Biomedical Engineering, Bogazici University.

Bahattin Koç is the Director of SU IMC and Professor of Manufacturing and Industrial Engineering at the SabancıUniversity. He received his Ph.D. and M.S. degrees in Industrial/Manufacturing Engineering from North Carolina State University in 2001 and 1997 respectively and his B.S. degree in Industrial Engineering from Istanbul Technical University, Istanbul, Turkey in 1993. He was an Associate Professor (Tenured) of Industrial and Systems Engineering at the University at Buffalo (UB) before joining to SabancıUniversity in 2010.

His research interests include additive manufacturing, heterogeneous object modeling and manufacturing, computational geometry for design and manufacturing,

nano/micro-scale manufacturing, three dimensional (3D) Bioprinting and product realization. He is the recipient of the Elginkan Foundation Science and Technology Award, Turkish Heart Association Award, "Most cited Author in Computer Aided Design" Award from Elsevier, UB STOR Inventor Award and UB Reifler Award. He has published more than 80 scientific publications (journal articles, book chapters and conference articles). Prof. Koç's research works have been supported by major national, international research agencies and organizations and companies such as the Scientific and Technological Research Council of Turkey (TÜBİTAK), the Turkish Ministry of Development, the European Research Council FP7, U.S. Army Medical Research and companies. Prof. Koç is an Associate Editor and a member of editorial boards of several journals in his research area. His recent research work related to 3D Organ Bioprinting was highlighted at several international and national TV channels (BBC, CNN Turk etc.) Newspapers and blogs.